IJISET - International Journal of Innovative Science, Engineering & Technology, Vol. 3 Issue 8, August 2016
ISSN (Online) 2348 – 7968 | Impact Factor (2015) - 4.332
www.ijiset.com

Polyaniline doped folic acid with morphologic like-plates and high crystallinity, synthesis and characterization

Vicente Lira Kupfer[1*], Cleiser Thiago Pereira da Silva[1], Nelson Luis de Campos Domingues[2], Murilo Pereira Moises[3], Andrelson Wellington Rinaldi[1]

[1]*(Laboratory of Materials Chemistry and Sensors - LMSen, State University of Maringá - UEM, 5790 Colombo Avenue, 87020-900, Maringá, PR, Brazil)*

[2]*(Laboratory of Catalysis and Biocatalysis Organic - LACOB, Federal University of the Grande Dourados - UFGD, Km 12 Dourados Itahum road, 79.804-970, Dourados, MS, Brazil)*

[3]*(Fede*ral Technological University of Paraná - UFTPR, *635 MarcílioSstreet, 86812-460, Apucarana, PR, Brazil)*

** Correspondence to: Laboratory of Materials and Sensors - LMSen, State University of Maringá, Maringá, Paraná, Brazil. Tel.: +55 44 3011 5280.*

E-mail address: vicente.kupfer@yahoo.com.br; or awrinaldi@uem.br

Abstract

The Polyaniline doped with folic acid (PAni/FA) was synthesized by chemical oxidative polymerization of aniline in emulsion acid solution using ammonium persulfate as an oxidant. The PAni/FA was prepared in different dilutions. The material obtained was a green powder and it was characterized by techniques of infrared spectroscopy (FTIR), UV-Vis spectroscopy, thermogravimetric analysis (TGA), conductivity (EIE) and the morphology of PAni/FA was characterized by SEM. The materials which were prepared with high concentrations of monomers presented small crystalinity than materials synthesized with small concentration of monomers. The conductivity is about $10^{-4}Scm^{-1}$ in the material with the highest monomer concentration and the conductivity is lower when the monomer concentration was reduced in polymerization solution. In addition, the materials proved soluble in organic solvents N-methyl, 2-pyrrolidinone (NMP), dimethyl sulfoxide (DMSO) and dimethyformamide (DMF).

Keywords: Polymer composites, PAni, folic acid, chemical polymerization, morphologic like-plates.

1. Introduction

Researchers all over the world still have great interest for Polyaniline (PAni), because this is one of the most promising conjugated polymers, especially for this properties such as electronic conductivity, optical characteristics, redox properties, environmental stability, facility of doping, stability when exposed to the air and in aqueous solutions, good biological compatibility and low costs of the monomers (Jun, Sim, and Choi 2015),(Li et al. 2016),(Zhu et al. 2016),(Liu et al. 2016). These characteristics make PAni vastly applicable in, sensors (Kumar and Yadav 2016),(Gavgani et al. 2016), supercapacitors (Maiti and Khatua 2014), (Chen 2016), antistatic cover, anticorrosion coating (Kazum and Kannan 2016), (Heydari et al. 2016).

PAni synthesis with nanometric or micrometers geometric shapes like flower (Yu et al. 2011), fibrous (Ho et al. 2009), (Fryczkowski et al. 2012), (Nath et al. 2013) spheres (Fan et al. 2013), (da Silva et al. 2013), sheets (J. Wang et al. 2008), (Haibin Zhang et al. 2009), (Wu et al. 2010), plates (J. Wang et al. 2009), *inter alia* is extensively described in the literature. The modulation of physical and chemical properties of these nanomaterials may be achieved by controlling the morphology and organization in the synthesis of the materials (J. Wang et al. 2008). Wang and co-works (X. Wang et al. 2010) have synthesized PAni with different morphologies (nanofibers, nanotubes, nanodisks and micromats) through emulsion route. Wei and co-works (Wei et al. 2013) have prepared a polymerization of aniline in the presence of carbon nanofibers (CFs) to fabricate ordered whisker-like PAni/CF with long cycle life for supercapacitors. The authors conclude that the morphology and the synergistic effect of the components are responsible for the excellent electrochemical performance. Zhang and co-works (Hongming Zhang et al. 2011) have prepared PAni films containing phosphonic acids with different numbers of (m) repeating $–CH_2CH_2O–$ units (m = 1–16). The side chain length of the dopant increase

the crystalline and electrical conductivity of PAni. Furthermore, mean particle size spherical of PAni morphology decreased when *m* value decreased from 16 to 1.

In this paper, we have synthesized PAni doped with folic acid (FA) by chemical reduction with ammonium persulphate (APS). The molar ratio of reactants was kept constant, and the dilution of the solution was increased synthesis, to produce plates-like polyaniline with high crystallinity.

2. Experimental Part

The aniline monomer (Aldrich, 99.5%) was previously distillated in nitrogen atmosphere with metallic zinc. Then distillated aniline (5 mMol) and the FA (5 mMol) were added in a reaction flask with determined amount of ultra pure water (Milli-Q) (50 mL, 100 mL and 200 mL). The solution was stirred during 30 min in low temperature (0ºC) to assure the formation of an emulsion. The initial pH observed for all solution was *ca.* 2.00.

Subsequently 10.0 mL of aqueous solution of APS (0.70 $molL^{-1}$) was slowly added (*ca.* 50 $\mu Lmin^{-1}$) into the mixture. Afterwards, the mixture was stirred for 12 h at temperature ~0.0^0C. After this, the precipitated material was filtered, washed abundantly with water, ethanol tree times and dried under vacuum (40.0^0C) for 48 h. The material obtained a dark-green powder named as PAni/AF#1 to materials synthesized in 50 mL of water, PAni/AF#2 in 100 mL, and PAni/AF#3 in 200 mL of water.

Major headings are to be column centered in a bold font without underline. They need be numbered. "2. Headings and Footnotes" at the top of this paragraph is a major heading.

3. Characterization

The spectroscopy measurements on the IR region (FTIR) were performed in KBr by using an equipment JASCO model 4100 on the region from 400 to 4000 cm^{-1} with a resolution of 4 cm^{-1}. The molecular absorbance spectra (UV-Vis) were carried out in a spectrophotometer UV-Vis Varian Cary 50. The polymer solutions were prepared through the solubilization of 0.1 gL^{-1} of the materials in N-methyl-2-pyrrolidone (NMP) and were observed on the region between 200 and 800 nm. The thermal stability of the polymers was evaluated through thermogravimetric analysis curves (TGA) by using a thermogravimetric analyzer Shimadzu model TA 50. The surface morphology was monitored by scanning electron microscopy (SEM) (JEOL 6830LV Microscope). X-ray diffractions patterns were recorded on a Shimadzu diffractometer (XDR-6000) using CuK_α radiation (1.5418 Å) at 30 mA and 40 kV, at a scanning rate of 2°min^{-1}.

The ageing of the polymer was carried out by storage in ambient conditions (RH = 45%, $T = 25^0$C). The conductivity measurements were carried out by using impedance data which were obtained by potenciostate/galvanostate Autolab Mod. 302 N, coupled to a frequency response analyser (FRA). The FRA measurements were executed by using a range between 1 Hz and 1 MHz bias was 0 V and sinusoidal voltage amplitude 100 mV. The experimental uncertainness data on resistance (*R*) and capacitance from the fitting process were within 2%. The conductivity was calculated by using Equation 1. (Girotto and Paoli 1999), (Rinaldi et al. 2005).

$$Rp = d / (A\sigma)$$

Equation 1

The conductivity measurements were performed on tablets prepared in a suitable mold Teflon® with a pressure of 3.0 tons. The conductivity measurements were performed in triplicate. When *d* is the thickness of the polymer film, *A* is the geometric area of the electrode and *Rp* is the resistance of the material determined in parallel with its geometric capacitance.

4. Results and discussion

During the initial synthesis process this was observed that the reactional mixture PAni and FA presented yellowish coloration because of the solubilization of FA. From the addition of the oxidant agent APS, the solution slowly became green, this green color is characteristic of the PAni. This was observed that the solutions which contained the smallest quantities of water (PAni/FA#1 and PAni/FA#2) presented the more intense colorations.

The Figure 1 presents the FTIR spectra for the PAni/HCl, Folic acid and the materials synthesized with different amounts of water. The peaks in 1580 cm^{-1} e 1485 cm^{-1} correspond to the stretching mode N=C and C=C respectively, including the stretching of both quinone and benzene rings of the PAni/HCl synthesized according to the literature (Yuping et al. 2010). The peaks in 1299 cm^{-1} and 1234 cm^{-1} are characteristic of the stretching vibrations C-N of the aromatic secondary amines and the peak in 1064 cm^{-1} is characteristic of the protonated PAni.

In the spectrum to the synthesized materials (PAni/FA#1, PAni/FA#2, PAni/FA#3) is observed both characteristic peaks of FA (1695 cm^{-1} and 1608 cm^{-1}) and protonated PAni (1113 cm^{-1}) indicating the effectiveness

of the achievement of PAni doped with FA. Another observation was that the characteristic peaks of the stretching C-N, from the protonated PAni, is displaced to a longer wavelength and this displacement is attributed to interactions existing between PAni and FA on the PAni/FA material when this is compared to the PAni/HCl.

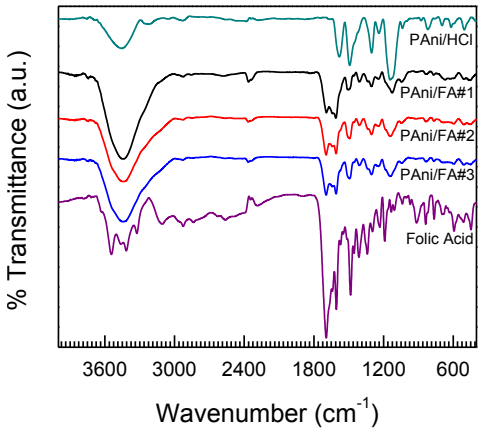

Figure 1 - FTIR spectra of PAni/HCl, PAni/FA#1, PAni/FA#2, PAni/FA#3, and Folic Acid.

The Figure 2 shows the absorption spectra on the UV-Vis region to synthesized materials and FA. In the PAni/FA#1 and PAni/FA#2 spectrum is possible to remark on the spectra the presence of electronic transitions in *ca.* 630 nm, that can be attributed to the transitions n-π* characteristics of PAni on the semiconductor status and can be related to the polaron transitions of the quinoide rings (Hsieh et al. 2010).

Confronting the FTIR results with the ones obtained from the UV-Vis spectra, this can be suggested that the processes of synthesis was better when is used the lowest volume of water (*i.e.* PAni/FA#1 and PAni/FA#2 solutions more concentrated in monomers).

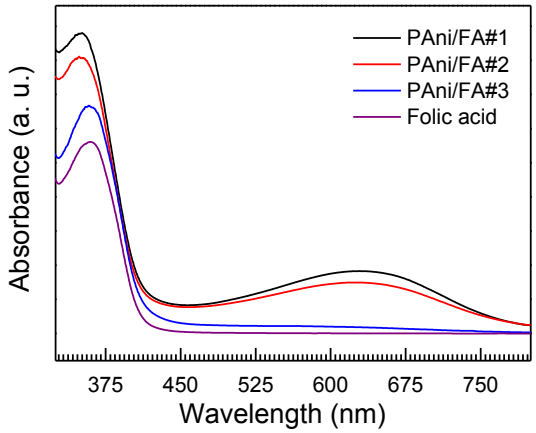

Figure 2 - UV-Vis spectra of resulting materials: PAni/FA#1; PAni/FA#2; PAni/FA#3; and FA.

For the material synthesized with the higher amount of solvent (water), which are: PAni/FA#3, the polaron transition which a characteristic of the quinoide rings (630 nm) of the PAni were not observed. According to the literature (Sedenková et al. 2009), this fact can be related to a decreasing of the proportions existing between both rings quinoide and benzene.

The thermal stabilities of materials are illustrated in the Figure 3. This was verified that pure materials PAni/HCl presents tree mass loss processes, which is consistent with the literature (Umare, Shambharkar, and Ningthoujam 2010), (Rather et al. 2013). The results of TG for the synthesized materials shows that the evaporation of the remaining solvent within the material is around 120^{o}C which corresponds to *ca.* 5% of the total mass of the material. The event observed on the interval of 120-225^{o}C can be attributed to the component glutamic acid, which breaks the bond with the FA structure (Vora et al. 2002). Increasing the temperature another event of mass loss happens in *ca.* 225-450^{o}C, where the 4-amino benzoic acid (PABA) is released from the FA, so the decomposition happens (Vora et al. 2002)(Biçak, Senkal, and Sezer 2005). From 450^{o}C till 600^{o}C the mass loss is related to the PAni residual decomposition. Moreover, the doped PAni with FA presents thermal stability increase when compared with FA (Fig. 3). This conclusion comes from the data of mass loss observed to PAni that loses 10% of mass in *ca.* 86^{o}C and the materials doped loses *ca.* 3%. These differences of the materials and FA can be explained through the existence of a synergistic effect between PAni and FA and this fact can increase the temperature loss.

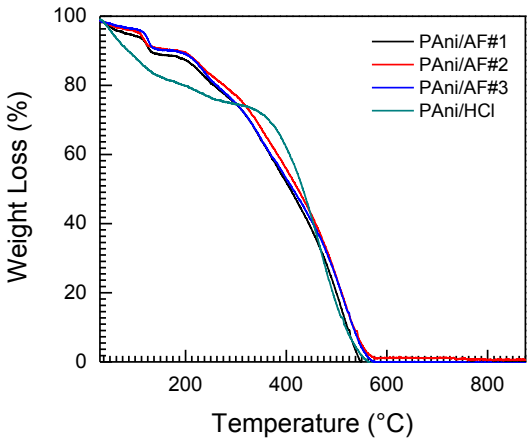

Figure 3 – TG curves of PAni/HCl, PAni/FA#1, PAni/FA#2 and PAni/FA#3. Heating rate of 10^{o}Cmin^{-1} and N_2 flow rate of 20 mLmin^{-1}.

The Figure 4 presents scanning electron micrograph (SEM) for the precursor and synthesized the materials. The PAni/HCl corresponds to a granular

uniform morphology as described on the literature (Roy, Anilkumar, and Prasad 2012).

The materials PAni/FA#1, PAni/FA#2, and PAni/FA#3, presents morphologic similarities, where the morphology of the materials suggest an evidence of the formation of plates associated to irregular particles. This proceeding can be attributed to the increasing of quantity of water in the emulsion providing the formation of lamellae. These structures can be attributed to the presence of FA on the material. Moreover, the presence of higher water amount makes the plates increase.

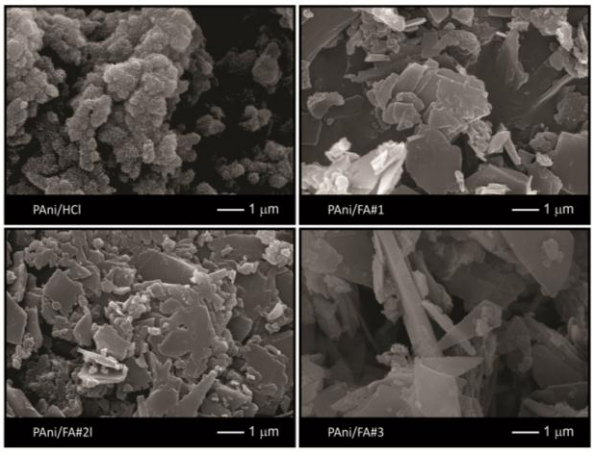

Figure 4 – Surface SEM micrographs of PAni/HCl, PAni/FA#1, PAni/FA#2 and PAni/FA#3.

The Figure 5 illustrates the X-ray diffraction analyses to PAni/HCl, folic acid and synthesized materials. Therefore, this is clearly that PAni/HCl diffractogram, Figure (5a) exhibited the broad and weak reflection in the range of 23–28°, which were the characteristic peak of amorphous PAni and in the Figure (5e) is presented the XRD results to crystalline folic acid (standard pattern number 29-1716– ICDD database).

The XRD results of the materials developed from this work reveals the presence of sharp and distinct peaks corresponded to folic acid indicating that PAni was doped with FA. These results corroborate to FTIR in SEM results. The increase in the crystallinity (relative of the PAni/FA#1) was calculated considering the ratio of the higher intensity signals (2Θ = 10.8; 12.9; 16.2; 26.6 and 27.1) and was found that structure organization of PAni/FA#2 and PAni/FA#3 increasing 5% and 17% respectively as shows in *inset* of Figure 5. This crystallinity increase is explained for higher water volum in this precursor solution resulting a more oriented material due to impingement differrence in the precipitation reaction, in other words, the increase of water amount indicated lower rate of contact between precursor molecules, resulting in more crystalline preciptaded. This is agreement of morphology found to this material that reveled more organized structure in material PAni/FA#2 and PAni/FA#3.

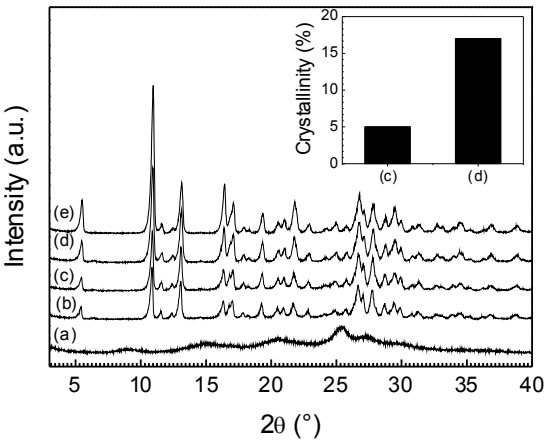

Figure 5. XRD results of (a) PAni/HCl, (b) PAni/FA#1, (c) PAni/FA#2, (d), PAni/FA#3 and (e) Folic Acid.

The electric conductivity measurements were performed through the spectroscopy of electrochemical impedance (EIE) and the results obtained for the conductivity measurements were calculated from the Equation 1. Both Rp values and the thickness of the respective samples are presented at Table 1. This is possible to note that the material PAni/FA#1 was the material which presented the higher conductivity value. This fact can be explained because this material, as Figure 1 and 2, showed the most characteristic of PAni and this compound (PAni/HCl) presents high conductivity. But the compounds PAni/FA#3, which presented most characteristic of FA, presented the small conductivity value. This can be explained because the FA isn't a conductor material.

Table1 – Values obtained of Rp, film thickness, once the electrode area of the conductor material tablets is about ($1.13x10^{-4}$ m^2).

Polymer	Rp	Thickness (m^2)	Conductivity (Scm^{-1})
PAni/HCl	2.13×10^3	2.8×10^{-4}	1.16×10^{-3}
PAni/FA#1	8.60×10^3	2.1×10^{-4}	2.16×10^{-4}
PAni/FA#2	2.61×10^4	1.9×10^{-4}	6.44×10^{-5}
PAni/FA#3	7.61×10^4	2.2×10^{-4}	2.56×10^{-5}

The materials identified as PAni/AF#1 and PAni/AF#2 were the ones that presented the best solubility in the following organic solvents: N-methyl-2-pyrrolidone (NMP), dimethylsulfoxide (DMSO) and N,N-dimethylformamide (DMF), nevertheless the solubility of these materials in aqueous media was inferior to the solubility than material identified PAni/FA#3. Again, this fact can be explained by using the Figure 1 and 2 where

presented the characteristics of these materials. The materials PAni/FA#1 and PAni/FA#2 presented more characteristics of PAni than material PAni/FA#3.

4. Conclusions

The synthesis of PAni doped with FA was performed through the chemical method by using APS as oxidant agent. Through the results described, we can suggested that is possible to synthesize the PAni by using FA as doping, but the concentration of the monomer (aniline) is essential to obtain PAni/FA with semi-conductor property.

Acknowledgments

The authors thank both the COMCAP – UEM for SEM analyses and the Brazilian agencies for fellowship CNPQ (Process: 577527/2008-8, 310820/2011-1), Fundação Araucária/PR and CAPES by financial support.

References

[1] C.S. Jun, B. Sim, H.J. Choi, Fabrication of electric-stimuli responsive polyaniline/laponite composite and its viscoelastic and dielectric characteristics, Colloids Surfaces A Physicochem. Eng. Asp. 482 (2015) 670–677. doi:10.1016/j.colsurfa.2015.07.014.

[2] W. Li, Y. Tian, C. Zhao, Q. Zhang, W. Geng, Synthesis of magnetically separable Fe3O4@PANI/TiO2 photocatalyst with fast charge migration for photodegradation of EDTA under visible-light irradiation, Chem. Eng. J. 303 (2016) 282–291. doi:10.1016/j.cej.2016.06.022.

[3] K. Zhu, Y. Gao, X. Tan, C. Chen, Polyaniline-Modified Mg/Al Layered Double Hydroxide Composites and Their Application in Efficient Removal of Cr(VI), ACS Sustain. Chem. Eng. (2016) acssuschemeng.6b00922. doi:10.1021/acssuschemeng.6b00922.

[4] Y. Liu, Y. Yang, L. Chen, H. Zhu, Y. Dong, N.S. Alharbi, A. Alsaedi, J. Hu, Efficient removal of U(VI) from aqueous solutions by polyaniline/hydrogen-titanate nanobelt composites, RSC Adv. 6 (2016) 56139–56148. doi:10.1039/C6RA10162C.

[5] R. Kumar, B.C. Yadav, Humidity sensing investigation on nanostructured polyaniline synthesized via chemical polymerization method, Mater. Lett. 167 (2016) 300–302. doi:10.1016/j.matlet.2016.01.082.

[6] J.N. Gavgani, A. Hasani, M. Nouri, M. Mahyari, A. Salehi, Highly sensitive and flexible ammonia sensor based on S and N co-doped graphene quantum dots/polyaniline hybrid at room temperature, Sensors Actuators, B Chem. 229 (2016) 239–248. doi:10.1016/j.snb.2016.01.086.

[7] S. Maiti, B.B. Khatua, Polyaniline integrated carbon nanohorn: A superior electrode materials for advanced energy storage, Express Polym. Lett. 8 (2014) 895–907. doi:10.3144/expresspolymlett.2014.91.

[8] W. Chen, Nano nickel oxide coated graphene/polyaniline composite film with high electrochemical performance for flexible supercapacitor, Electrochim. Acta. 211 (2016) 1066–1075. doi:10.1016/j.electacta.2016.06.026.

[9] O. Kazum, M.B. Kannan, Optimising parameters for galvanostatic polyaniline coating on nanostructured bainitic steel, Surf. Eng. 32 (2016) 607–614. doi:10.1080/02670844.2015.1108071.

[10] M.H. Heydari, H. Zebhi, K. Farhadi, P.N. Moghadam, Electrochemical synthesis of nanostructure poly(3-aminobenzoic acid), polyaniline and their bilayers on 430SS and their corrosion protection performances, Synth. Met. 220 (2016) 78–85. doi:10.1016/j.synthmet.2016.04.019.

[11] X. Yu, H. Fan, H. Wang, N. Zhao, X. Zhang, J. Xu, Self-assembly of flower-like polyaniline-polyvinyl alcohol multidimensional architectures from 2D petals, Mater. Lett. 65 (2011) 2812–2815. doi:10.1016/j.matlet.2011.05.116.

[12] K.S. Ho, Y.K. Han, Y.T. Tuan, Y.J. Huang, Y.Z. Wang, T.H. Ho, T.H. Hsieh, J.J. Lin, S.C. Lin, Formation and degradation mechanism of a novel nanofibrous polyaniline, Synth. Met. 159 (2009) 1202–1209. doi:10.1016/j.synthmet.2009.02.047.

[13] R. Fryczkowski, M. Gorczowska, B. Fryczkowska, J. Janicki, Morphology of highly porous conducting polyaniline nanofibres synthesized in a multi-phase system, Fibers Polym. 13 (2012) 703–708. doi:10.1007/s12221-012-0703-x.

[14] C. Nath, A. Kumar, R. Fryczkowski, M. Gorczowska, B. Fryczkowska, J. Janicki, Effect of temperature and magnetic field on the electrical transport of polyaniline nanofibers, Fibers Polym. 113 (2013) 703–708. doi:10.1007/s12221-012-0703-x.

[15] H. Fan, N. Zhao, H. Wang, X. Li, J. Xu, Preparation and electrochemical property of tremella-like polyaniline microspheres by a template-free method, Mater. Lett. 92 (2013) 115–118. doi:10.1016/j.matlet.2012.10.081.

[16] C.T.P. da Silva, M.D. dos S. Neto, V.L. Kupfer, S.L. de Oliveira, N.L. de C. Domingues, A.W. Rinaldi, Electrochemical synthesis of polyaniline microspheres in alkaline media, Mater. Lett. 100 (2013) 303–305. doi:10.1016/j.matlet.2013.02.094.

[17] J. Wang, J. Wang, Z. Yang, Z. Wang, F. Zhang, S. Wang, A novel strategy for the synthesis of polyaniline nanostructures with controlled morphology, React. Funct. Polym. 68 (2008) 1435–1440. doi:10.1016/j.reactfunctpolym.2008.07.002.

[18] H. Zhang, J. Wang, Z. Wang, F. Zhang, S. Wang, A novel strategy for the synthesis of sheet-like polyaniline, Macromol. Rapid Commun. 30 (2009) 1577–1582. doi:10.1002/marc.200900228.

[19] Y. Wu, L. Huang, Z. Liu, Z. Yang, Facile preparation of curved polymer composite nanosheets, Polymer (Guildf). 51 (2010) 3075–3082. doi:10.1016/j.polymer.2010.04.056.

[20] J. Wang, J. Wang, Z. Dai, Z. Wang, F. Zhang, Preparation of polyaniline microplates via a novel template-free method, Synth. Met. 159 (2009) 1583–1588. doi:10.1016/j.synthmet.2009.04.020.

[21] X. Wang, Y. Li, Y. Zhao, J. Liu, S. Tang, W. Feng, Synthesis of PANI nanostructures with various morphologies from fibers to micromats to disks doped with salicylic acid, Synth. Met. 160 (2010) 2008–2014. doi:10.1016/j.synthmet.2010.07.030.

[22] J. Wei, J. Zhang, Y. Liu, G. Xu, Z. Chen, Q. Xu, Controlled growth of whisker-like polyaniline on carbon nanofibers and their long cycle life for supercapacitors, RSC Adv. 3 (2013) 3957. doi:10.1039/c3ra23040f.

[23] H. Zhang, J. Lu, X. Wang, J. Li, F. Wang, From amorphous to crystalline: Practical way to improve electrical conductivity of water-borne conducting polyaniline, Polymer (Guildf). 52 (2011) 3059–3064. doi:10.1016/j.polymer.2011.02.031.

[24] E.M. Girotto, M. a De Paoli, Transporte de massa em polímeros intrinsecamente condutores: importância, técnicas e modelos teóricos, Quim. Nova. 22 (1999) 358–368. doi:http://dx.doi.org/10.1590/S0100-40421999000300014.

[25] A.W. Rinaldi, R. Matos, A.F. Rubira, O.P. Ferreira, E.M. Girotto, Electrical, spectroscopic, and thermal properties of blends formed by PEDOT, PVC, and PEO, J. Appl. Polym. Sci. 96 (2005) 1710–1715. doi:10.1002/app.21637.

[26] D. Yuping, W. Guangli, L. Xiaogang, J. Zhijiang, L. Shunhua, L. Weiping, On the correlation between structural characterization and electromagnetic properties of doped polyaniline, Solid State Sci. 12 (2010) 1374–1381. doi:10.1016/j.solidstatesciences.2010.05.013.
[27] T.H. Hsieh, K.S. Ho, X. Bi, C.H. Huang, Y.Z. Wang, Y.K. Han, Z.L. Chen, C.H. Hsu, P.H. Li, Y.C. Chang, Effects of [SDS]/[H2O] molar ratio on the electromagnetic properties of polyaniline/maghemite nanocomposites, Synth. Met. 160 (2010) 1609–1616. doi:10.1016/j.synthmet.2010.05.023.
[28] I. Sedenková, M. Trchová, J. Stejskal, J. Prokes, Solid-state reduction of silver nitrate with polyaniline base leading to conducting materials, ACS Appl. Mater. Interfaces. 1 (2009) 1906–1912. doi:10.1021/am900320t.
[29] S.S. Umare, B.H. Shambharkar, R.S. Ningthoujam, Synthesis and characterization of polyaniline-Fe3O4 nanocomposite: Electrical conductivity, magnetic, electrochemical studies, Synth. Met. 160 (2010) 1815–1821. doi:10.1016/j.synthmet.2010.06.015.
[30] M.S. Rather, K. Majid, R.K. Wanchoo, M.L. Singla, Synthesis, characterization, and thermal study of polyaniline composite with the photoadduct of potassium hexacyanoferrate (II) involving hexamine ligand, J. Therm. Anal. Calorim. 112 (2013) 893–900. doi:10.1007/s10973-012-2609-7.
[31] A. Vora, A. Riga, D. Dollimore, K.S. Alexander, Thermal stability of folic acid, Thermochim. Acta. 392-393 (2002) 209–220. doi:10.1016/S0040-6031(02)00103-X.
[32] N. Biçak, B.F. Senkal, E. Sezer, Preparation of organo-soluble polyanilines in ionic liquid, Synth. Met. 155 (2005) 105–109. doi:10.1016/j.synthmet.2005.06.010.
[33] A.S. Roy, K.R. Anilkumar, M.V.N.A. Prasad, Studies of AC conductivity and dielectric relaxation behavior of CdO-doped nanometric polyaniline, J. Appl. Polym. Sci. 123 (2012) 1928–1934. doi:10.1002/app.34696.